Steel and Composite Structures, Vol. 5, No. 5 (2005) 375-394 375
DOI: http://dx.doi.org/10.12989/scs.2005.5.5.375

A new base plate system using deformed reinforcing bars for concrete filled tubular column

Yong-Myung Park†

Department of Civil Engineering, Pusan National University, 30 Jangjeon-dong, Geumjeong-gu, Busan 609-735, Korea

Won-Sup Hwang‡

Department of Civil Engineering, Inha University, 253 Yonghyun-dong, Nam-gu, Incheon 402-715, Korea

Tae-Yang Yoon‡† and Min-Oh Hwang‡‡

Civil Engineering Research Team, Research Institute of Industrial Science and Technology, 79-5 Youngcheon, Dongtan, Hwaseong, Gyeonggi-do, 445-813, Korea

(Received August 24, 2004, Accepted March 25, 2005)

Abstract. An experimental study was conducted to develop a new base plate anchorage system for concrete filled tubular column under an axial load and a moment. The column was connected to a concrete foundation using ordinary deformed reinforcing bars that are installed at the inside and outside of the column. In order to investigate the moment resisting capacity of the system, horizontal cyclic loads are applied until the ultimate condition is reached with the axial load held constant. To derive a design method for moment resisting capacity, the reinforced concrete section approach was investigated with the assumption of strain compatibility. The results by this approach agreeded well with those of experiments when the bearing pressure of confined concrete and tangent modulus of steel bars are assumed appropriately. Also, it was found that the column interaction curve can be used to predict the yield strength of the base plate system.

Key words: column base plate; reinforcing bar anchor; moment resisting capacity; reinforced concrete section method; interaction curve.

1. Introduction

The role of column base plate is to transfer the load from a steel column to the supporting concrete foundation. The column base plates may be subjected to three types of loading depending on the eccentricity of the load, namely, (1) axial load only, (2) axial load plus a relatively small moment, (3) axial load plus a relatively large moment. In the first case and sometimes in the second case, the entire area of base plate is under compressive pressure. In this situation, nominal anchorage will be sufficient

†Associate Professor, Corresponding author, E-mail: ympk@pusan.ac.kr
‡Professor
‡†Ph. D.
‡‡Senior Researcher

to hold the base plate in position. However, when the eccentricity of loading becomes larger, resulting in a relatively large moment, lifting of the base plate will occur. In this case, anchor bolts are necessary to maintain equilibrium. Since base plates are not rigid, bending of the base plate occurs so that the bearing stress developed in the concrete foundation is by no means uniform.

A number of studies have been conducted to investigate the behavior of the base plate and the bearing pressure under concentrically loaded column. Among those, DeWolf (1978) presented a noteworthy experimental results on the behavior of base plates subject to an axial load at the central area, resulting in base plate bending. The major factors that affect the bearing stresses in the concrete were assumed to be the concrete strength, the plate thickness, and the ratio of the concrete to plate area, which affects confinement and, consequently, the triaxial stress state in the concrete. For the remaining researches, it is recommended to refer to the published material (AISC 1990).

Limited work has been done for base plates which are designed to resist both an axial load and a moment. Salmon *et al.* (1957) first analytically studied the moment-rotation characteristics of column anchorages. Their method was established to estimate the upper and lower bound ultimate moments for anchorages with the axial load held constant. DeWolf and Sarisley (1980) conducted a series of tests of base plates with moments. In the tests, small-size hollow rectangular columns were used and the parameters included are the plate thickness, the anchor bolt size, and the ratio of eccentricity. They found that the behavior at failure was not always consistent with the assumption used in the present design approaches. Thambiratnam and Paramasivam (1986) also performed a similar experimental study of base plates with hollow rectangular column subject to eccentric loads. Their parameters also included the ratio of eccentricity and thickness of the base plates. They concluded that the strength of anchorage system is substantially dependent on the flexibility of the base plate and eccentricity of loading. On the other hand, some computational approaches on the base plate were also performed to evaluate the ultimate behavior of the base plate taking into account the main parameters of the problem (Stamatopoulos and Ermopoulos 1997, Kontoleon *et al.* 1999).

The present study aims to develop a new anchorage system for steel piers which may undergo heavy and large eccentric loads due to traffic load or earthquake excitations while the previous studies were focused on the lightly loaded column. The conventional anchorage system of steel pier consists of the double base plate, large-size anchor bolts, and an anchor frame to withstand pulling-out force as shown in Fig. 1. In the authors' survey, Kitada *et al.* (1998) first performed an experimental study to assess the ultimate strength of the conventional base plate for steel pier with hollow rectangular column and suggested that the steel pier anchorage system can be designed by the reinforced concrete section method.

In the present study, a new anchorage system for concrete filled tubular piers that uses deformed bars to transfer the loads from the column to the concrete foundation instead of anchor bolts. The feature of proposed anchorage system is shown in Fig. 2. in which deformed bars are installed at the inside of the column by utilizing the filling concrete. Together with the inside bars, the deformed bars are installed at the outside of the column, which are fixed by nuts at base plate and serve as anchor bolts in the conventional system. The reinforcing bars are self-anchored into the foundation by bond characteristics, thus simplification of anchor structure will be possible to be an economical solution.

Presented herein are the results of an experiment to investigate the structural integrity and moment resisting capacity of the proposed anchorage system with an axial load and cyclic moment. From the test, the proposed system turned out to exhibit excellent moment-resisting capacity. To derive a design method for moment-resisting capacity, the reinforced concrete section approach was investigated. Also, column interaction curve was examined to investigate the applicability of the curve to predict the bending strength of the base plate system.

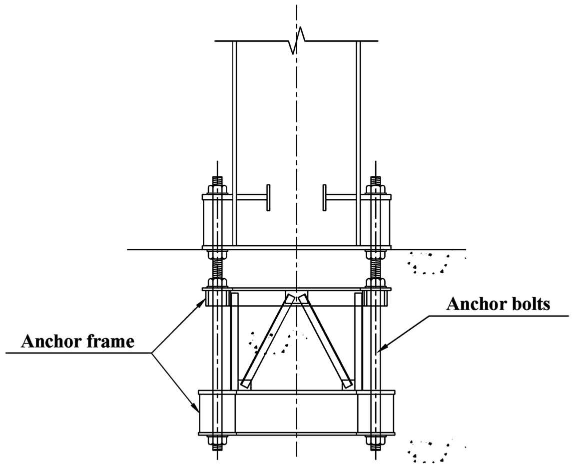

Fig. 1 Conventional anchor system

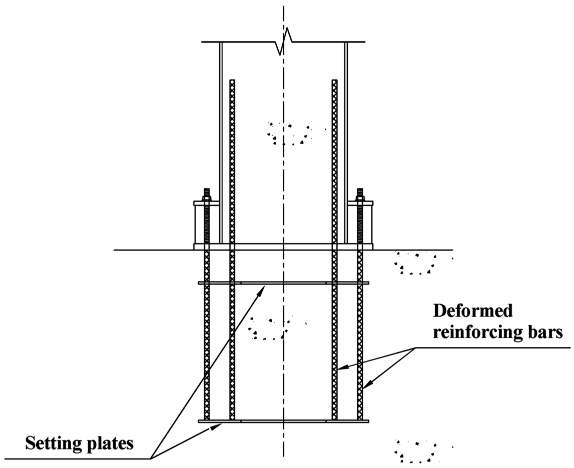

Fig. 2 Proposed anchor system

2. Structural experiment

2.1. Test specimen

In order to investigate the performance of a new base plate anchor system for steel pier using deformed bars, a steel column with sufficient rigidigy was designed so that the failure of reinforcing bars comes before that of the column. A circular column was adopted in this study due to its applicability in view of aesthetic point. The overall configuration of test specimen is shown in Fig. 3. The size of circular steel column is ϕ600×15 mm which corresponds to about 1/3 scale of common size of steel pier. The yield strength f_y of steel column is assumed as 32 kN/cm^2. Concrete was poured inside of the column to the full height. Thus, the concrete filled column is expected to have sufficient stiffness not to fail until the deformed bars arrive at the ultimate condition.

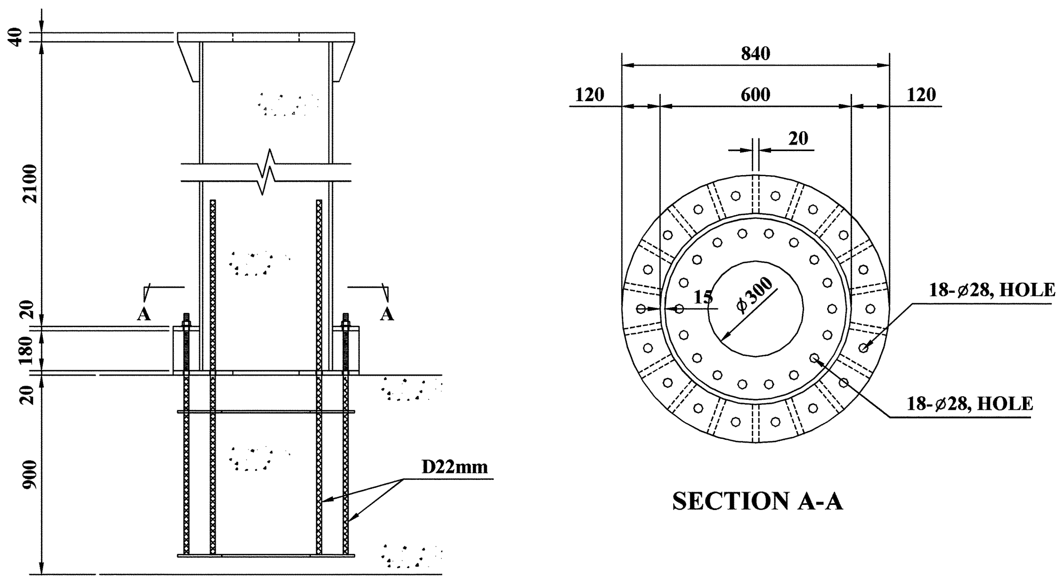

Fig. 3 Configuration of test specimen (unit: mm)

The size of concrete footing is 2.2 m width, 3.2 m length and 0.9 m thickness. The design strength of concrete used for column fill and foundation concrete is assumed as 2.65 kN/cm^2. The reinforcing bars of 22 mm diameters are installed each direction at the top and bottom of foundation with a spacing of 125 mm and a cover thickness of 50 mm. The reinforcement ratio amounts to 0.007 for both directions.

The base plates used for lightly loaded column in the previous researches (DeWolf and Sariley 1980, Thambiratnam and Paramasivam 1986) are single plates without stiffening ribs or brackets between column and base plates. Such base plates are not likely to withstand a heavy horizontal loads such as steel pier. Therefore, the base plate system in this study is designed as a double plate system which is composed of upper plate, lower plate and vertical ribs between upper and lower base plates as shown in Fig. 3. This type of base plate system is expected to carry heavy loads to the concrete foundation without excessive flexural deformation of the cantilevered part. The thickness of upper and lower base plate was determined by the plate theory for an individual part partitioned by vertical ribs. The boundary condition of a partitioned plate was assumed as three edges simply supported and one edge free. Then, the thickness of upper and lower plate was determined from equivalent pressure by anchor bars and concrete bearing pressure, respectively. The thickness of vertical ribs was determined by assuming them as columns subject to concrete bearing pressure or vertical force by anchor bolts. From the assumed calculation, 20 mm thick plates are selected for the upper, lower base plates and vertical ribs.

To connect column and foundation, eighteen deformed reinforcing bars of nominal diameter of 22 mm were installed at the inside of the column. They were self-anchored into the concrete filled column and concrete foundation. The embedment length of the deformed bars was determined as $l_d = 80$ cm based on the ACI code (2002) by assuming the nominal yield strength of reinforcing bars f_y as 35 kN/cm^2. Also, eighteen deformed reinforcing bars of the same diameter were installed at the outside of the column. The upper part of the outside bar was thread-rolled after forging and fixed by nut at the upper base plate such as the conventional base plate system as shown in Fig. 2. The threaded portion of the bars did not extend into the concrete. The lower part was also self-anchored into the concrete foundation such as the inside bars. The nuts were hand-tightened prior to the start of the tests.

Table 1 Strength of materials

Material \ Strength	Yield strength	Ultimate strength
Concrete	-	3.14 kN/cm^2
Steel	40.0 kN/cm^2	57.5 kN/cm^2

Tests were performed to evaluate material strength of the deformed bar and concrete. The average strength of the steel bar and concrete from UTM tests for three specimens is given in Table 1. From the tests, the strength of both concrete and reinforcing bars exceed the design strength.

2.2. Test setup and instrumentation

The concrete footing was fixed to the reaction bed by twelve anchor bolts of 50 mm diameter along the four edges. The test setup is shown in Fig. 4. Two 1,000 kN actuators were installed to apply axial load via loading beam and 2,000 kN actuator was installed at the loading beam to apply horizontal loads. The distance between the horizontal actuator and the base plate was 3 m.

The instrumentation is shown in Fig. 5. Displacement transducers were installed at each three points of the column and concrete foundation to measure the horizontal displacements. Also, strain gauges were installed at the inside and outside bars. For the inside bars, three gauges were installed at the upper, mid-height, and lower point of each bar in the concrete foundation. For the outside bars, which serve as anchor bolts in conventional base plate system, four strain gauges were installed at each bar,

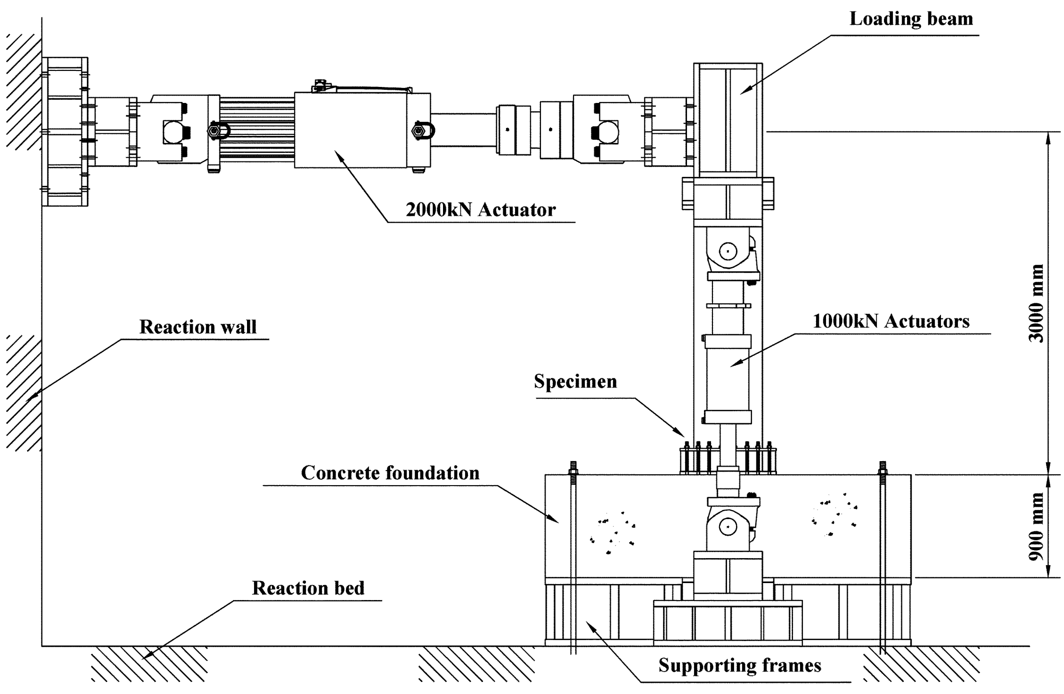

Fig. 4 Configuration of test setup

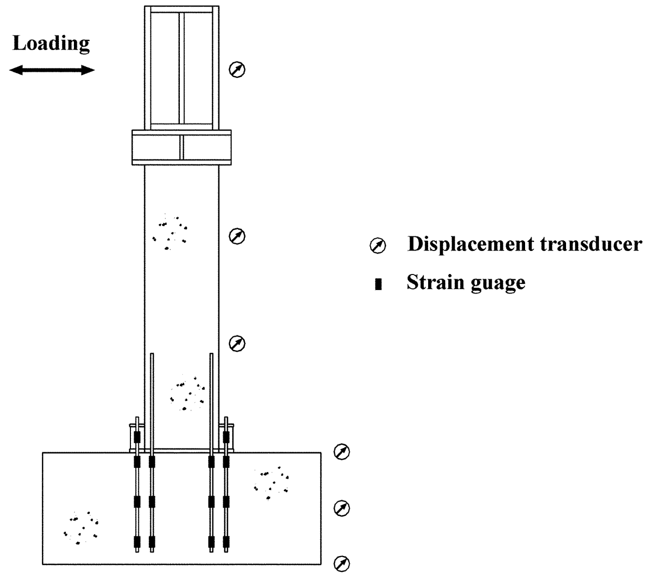

Fig. 5 Instrumentations

that is, a gauge at exposed point between the upper and lower base plate and three gauges for embedded part at the same level of the inside bars as shown in Fig. 5. The strain gauges are installed at the half area of the whole bars by considering symmetry.

2.3. Loading history

As shown in Fig. 6, test specimen was axially loaded by 1,180 kN which amounts to about 1/6 nominal yield strength of column to account for the usual dead load of a bridge super-structure. While maintaining the axial compressive loading constant, horizontal load was cyclically loaded with

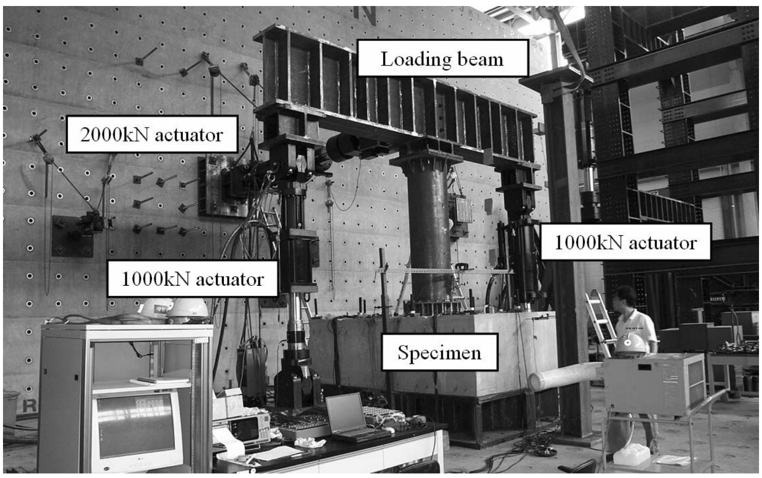

Fig. 6 Testing scene

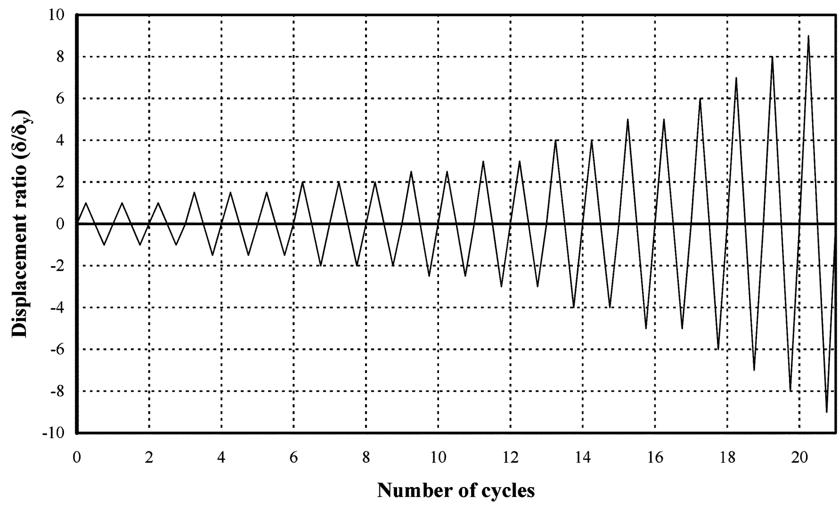

Fig. 7 Cyclic loading sequence

increasing amplitude until failure. Two 1,000 kN actuators were used to introduce an axial loading by force control and 2,000 kN actuator was used for a horizontal loading by displacement control, respectively. For the convenience of representation, the direction of the reversal load will be designated as north point for reaction wall side and south point for the opposite direction.

When the exposed outside bars at south and north points reached nominal yield strength of 35 kN/cm^2, it is considered the horizontal displacement at the level of horizontal actuator is yield displacement denoted as δ_y. The displacement δ_y was expected as 22 mm and the corresponding horizontal load was 355 kN from several preliminary loadings within elastic range. Thereafter, the reversal horizontal load was applied by displacement control in the sequence of ±1.0 δ_y, ±1.5 δ_y, ±2.0 δ_y, ±2.5 δ_y, ±3.0 δ_y, ±4.0 δ_y, ±5.0 δ_y.... The loading sequence is shown in Fig. 7 in which three cycles for the range of 1.0~2.0 δ_y, two cycles for 2.5~5.0 δ_y, and one cycle for the range beyond 5.0 δ_y were applied. The test was finished when the horizontal displacement reached to about 9.0 δ_y due to severe fracture of the concrete foundation at the vicinity of the column base plate.

2.4. Investigation of behaviors

2.4.1. Load-displacement curve

The hysteretic curve of load-displacement at the level of horizontal actuator is shown in Fig. 8. The enveloped curves are also depicted in Fig. 9. It is acknowledged from the curves in Fig. 8 and Fig. 9 that the anchorage system shows a symmetric behavior against reversal loadings.

When the horizontal load reached about 400 kN, the outer bars at north and south points arrived at yield stress of 40.0 kN/cm^2. It is observed from Fig. 9 that the slopes of the curves start to descend minutely from this load level due to yield of the outer bars. Also, the yield load of the anchor system is determined as 540 kN as shown in Fig. 9 and the corresponding moment is 1,620 kN · m. Therefore, the yield load of the anchor system amounts to 1.35 times of 400 kN when the outer bars first yielded. This can be explained by the fact that the adjacent outer bars and inside bars endure the additional moment after the outer bars at north and south points yield.

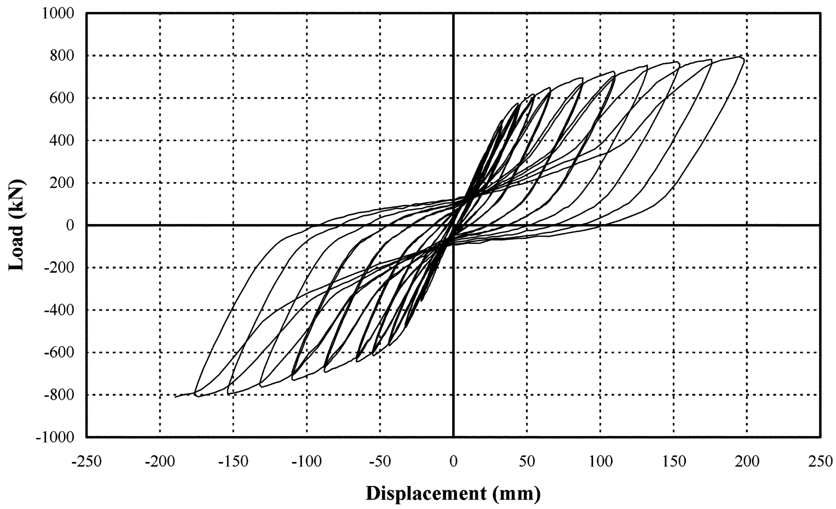

Fig. 8 Hysteretic curve for horizontal load-displacement

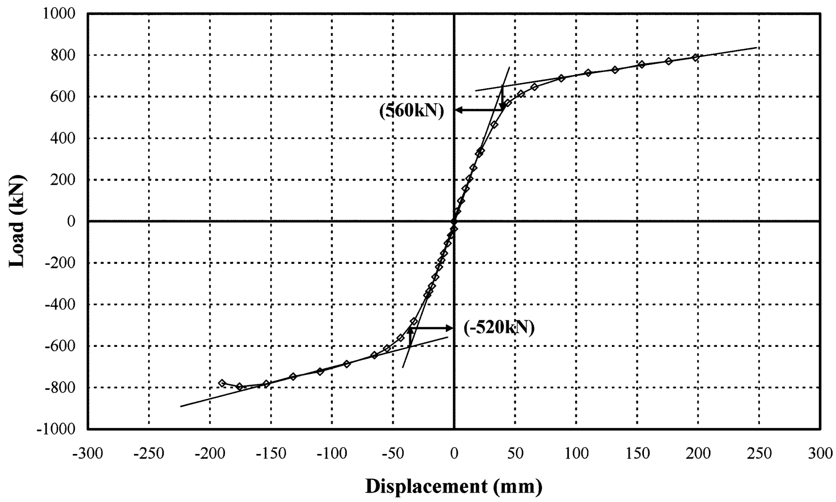

Fig. 9 Enveloped curve from hysteretic curve

During the test, gaps between the outer bar nuts and the upper base plate were observed when the horizontal displacement arrived at 2 δ_y due to plastic elongation of the bolt shanks and they increased as the horizontal load increases. The concrete crack around the base plate was observed when horizontal displacement exceeds 7 δ_y and the corresponding force is about 750 kN. The ultimate load is determined as 800 kN as shown in Fig. 9 and this is about 1.5 times of the yield load of the anchor system.

From the tests, it is acknowledged that the proposed anchor system has sufficient displacement ductility for moment resisting capacity and excellent recovery performance. The proposed system showed similar cyclic behavior with the conventional base plate system with a hollow steel pier conducted by Kitada *et al.* (1998). However, the hysteretic curve in this study is wider than that of the conventional system during the repeated loadings. This is considered that the anchor bolts can not resist tensile force when the gaps come from plastic elongation of the bolts in the conventional system while the inside bars in the proposed system can undertake the tensile force until the gaps between outer bar nuts and base plate get to close. Therefore, it is anticipated that the proposed system exhibits a higher energy absorbing capacity than the conventional system due to the existence of inside bars.

2.4.2. Strains of deformed bars

The hysteretic load-strain curves of the outer bars at south and north points which undergo maximum stresses are depicted in Fig. 10 and Fig. 11, respectively. First, Figs. 10(a) and 11(a) are the curves at the exposed level, i.e., at the base plate location. It is acknowledged that the maximum strains at north and south points are symmetric and the outer bars mainly endure tensile load since they are anchored by nuts. Figs. 10(b) and 11(b) are the strain curves at the upper level of the concrete foundation. These curves illustrate that the outer bars are effective for a tensile load but they are less effective for compression. Figs. 10(c) and 11(c) are the strain curves at mid-height level of the foundation. It is acknowledged that the bars are effective for both tension and compression while they are not effective for compression at the surface level of the foundation. Figs. 10(d) and 11(d) are strain curves at lower level of the foundation.

For the inside bars, the hysteretic curves at south and north points are shown in Fig. 12 and Fig. 13, respectively. Figs. 12(a) and 13(a) are the strains at the upper level of the concrete foundation. Here, it is recognized that the inside bars are effective for both tension and compression while the outside bar was only effective for tension at this level. This comes from the difference of anchoring mechanism, that is, the inside bars are embedded into concrete filled column while the outer bars are anchored by

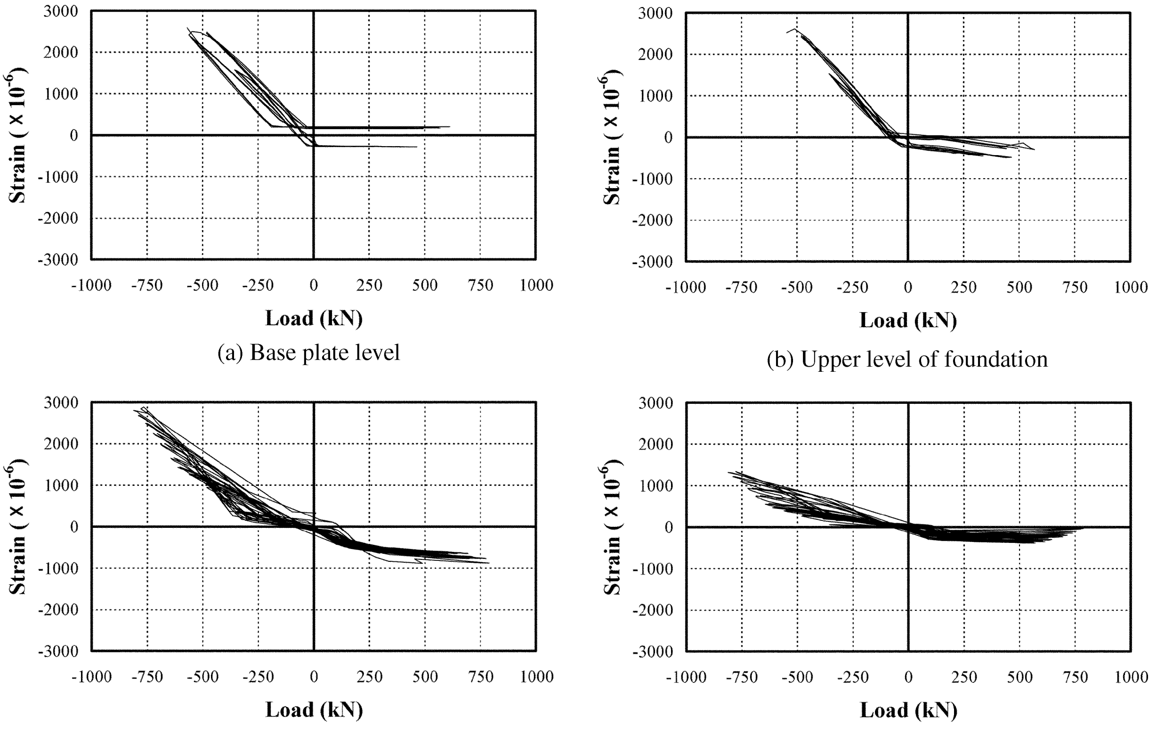

(a) Base plate level

(b) Upper level of foundation

(c) Mid-height level of foundation

(d) Lower level of foundation

Fig. 10 Strains of outside bar at South point

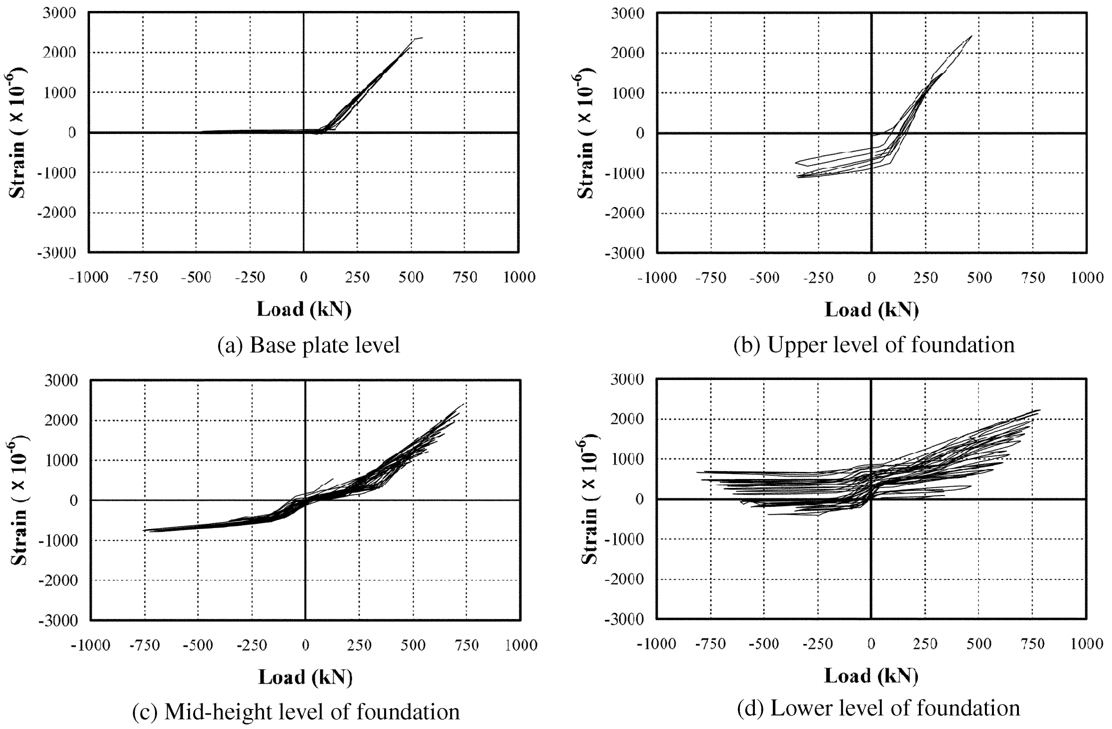

(a) Base plate level
(b) Upper level of foundation
(c) Mid-height level of foundation
(d) Lower level of foundation

Fig. 11 Strains of outside bar at North point

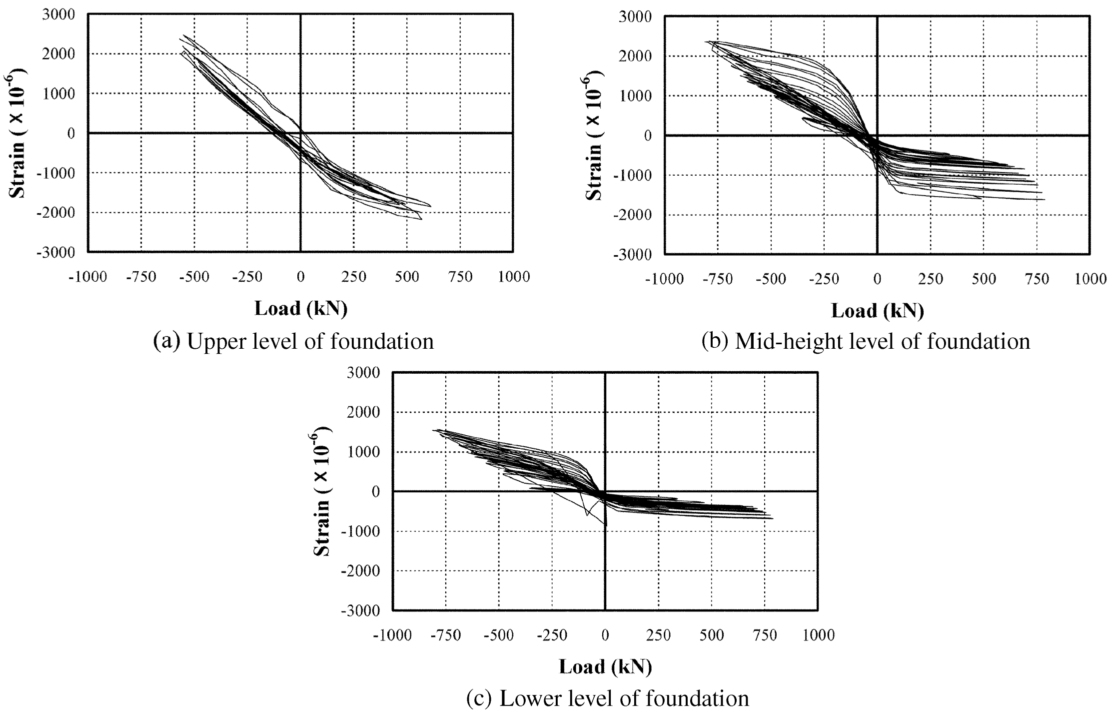

(a) Upper level of foundation
(b) Mid-height level of foundation
(c) Lower level of foundation

Fig. 12 Strains of inside bar at South point

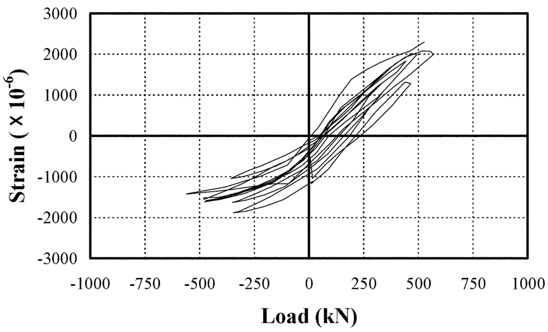

(a) Upper level of foundation

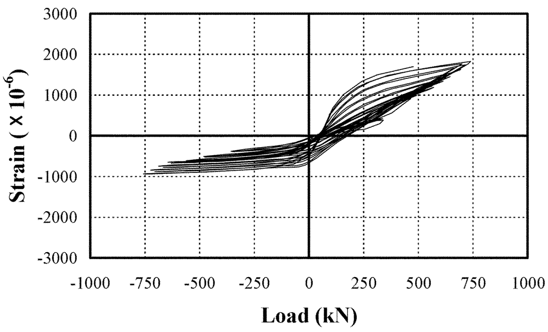

(b) Mid-height level of foundation

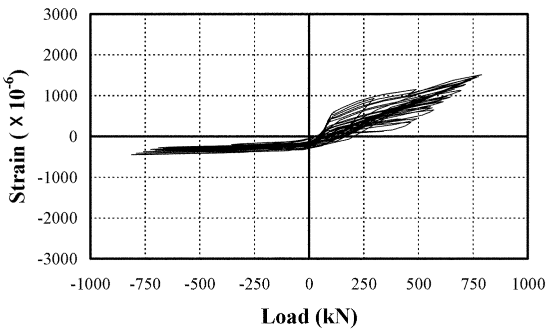

(c) Lower level of foundation

Fig. 13 Strains of inside bar at North point

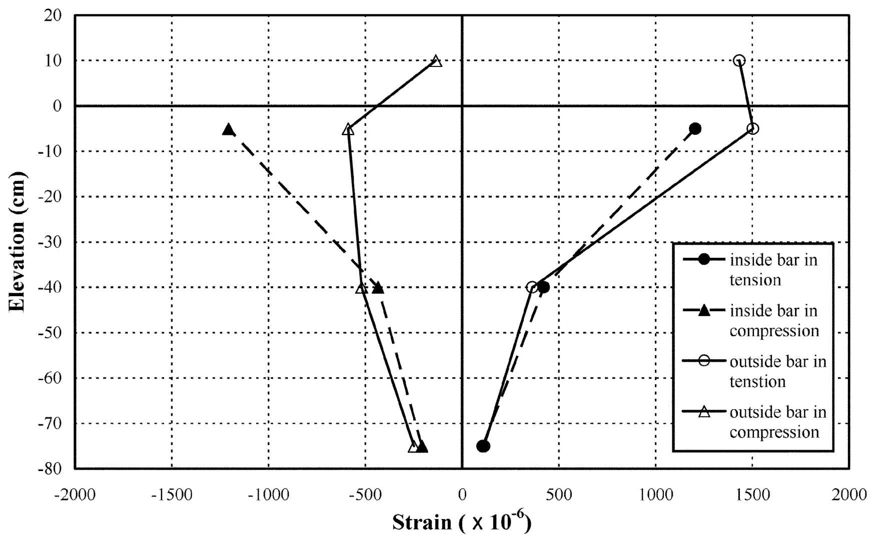

Fig. 14 Bar strain distribution

nuts. Figs. 12(b) and 13(b) are the strains at mid-height level of the foundation. It is recognized that the strain curves of these bars in tensile status are somewhat different with other cases. The reason for this can be explained by the gaps that occur between the outer bar nuts and the base plate when horizontal displacement exceeds 2 δ_y as mentioned previously. In other words, the inside bars solely undertake the tensile force until the gaps get to close. Figs. 12(c) and 13(c) are the strains at the lower level of the foundation.

The strains of the inside and outside bars along the bar elevation for horizontal displacement of 1.0 δ_y are also depicted in Fig. 14. It can be acknowledged from the figure that the inside bars are effective for both tension and compression while the outer bars are primarily effective for tension especially at the surface level. Also, the tensile strains of the inside bars are not so less than those of the outer bars. This implies that the inside bars take an important role to resist moment.

3. Design of base plate system

3.1. Review of the present method

Two general approaches, i.e., the working stress method and the ultimate strength method, exist for the design of base plates subject to axial load with moment (Gaylord and Gaylord 1972). The first method is based on the behavior assumed at the design or service load; the second method is based on the assumed behavior at ultimate load. DeWolf and Sarisley (1980) conducted a series of tests for base plates subject to moments and axial loads. They compared their experimental data to both approaches, and concluded that either could be used satisfactorily in design for their limited range of tests.

Thereafter, the Load and Resistance Factored Design method was introduced in AISC manual (1986) that may be used as an alternative to the working stress method. The method simply translated the working stress method into an equivalent limit state design format. In other words, it is actually based on the assumptions of elastic behavior with appropriate modifications to the load and stress.

The two principal approaches will be briefly reviewed and a design approach to evaluate moment resisting capacity of the proposed base plate system will be investigated.

3.1.1. Working stress method

In the working stress method, the bearing stress distribution in the concrete and anchor bolt stress are assumed to be elastic as shown in Fig. 15(a). The variable A_s is the total area of anchor bolts on the

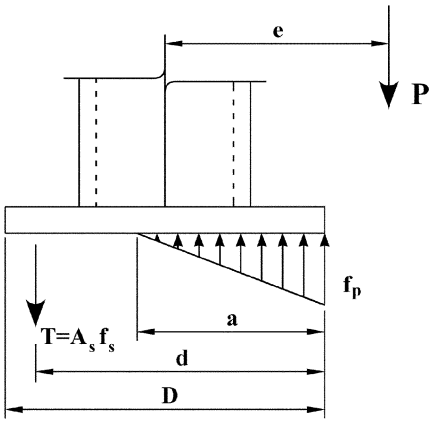

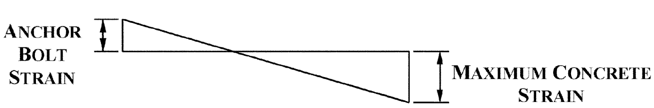

Fig. 15 Stress and strain distribution for working stress method

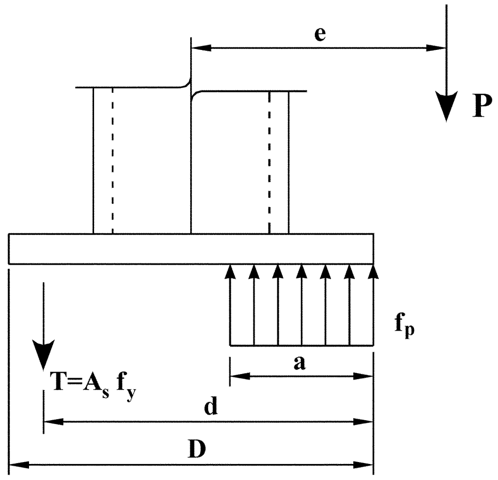

Fig. 16 Stress distribution for ultimate strength method

tension side; f_s is stress in the anchor bolts; f_p is maximum compressive bearing stress of concrete; P is applied axial force and M is moment. Given the axial load, the moment, and the plate dimensions, three unknowns exist, T, a and f_p where a is distance to neutral axis. An approach to finding these is to set f_p equal to the allowable value at a service load and then use the static equilibrium equations to find T and a, i.e., the sum of the vertical forces and sum of the moments must equal to zero (Gaylord and Gaylord 1972). For the third equation, a strain compatibility as shown in Fig. 15(b) can be applied so that the values of T is dependent on f_p. This is actually not consistent with the plate deformations because the base plate is not rigid.

3.1.2. Ultimate strength method

The ultimate strength method is based on the assumption that the anchor bolts are yielding and that the nonlinear concrete bearing stress distribution at failure can be replaced with an equivalent rectangular stress block as shown in Fig. 16. It is generally assumed that $f_p = 0.85 f_c'$, which corresponds to the basic value utilized in the design of reinforced concrete beams and columns (ACI 2002). This, however, neglects the favorable effects of the confinement that exists in the base plates positioned on the concrete foundations of greater area. In this method, two unknowns exist: the compression zone width a and either the eccentricity or axial force. They may be determined from two equilibrium equations.

3.2. Reinforced concrete section approach

3.2.1. Algorithm

The behavior of the concrete foundation for steel base plate is analogous to that of the reinforced concrete column. The essential difference between the two cases is the flexibility of the base plate. For unstiffened base plate connection, it is not correct to assume a linear strain distribution due to bearing at the concrete plate interface, i.e., plane sections do not remain plane.

Another important difference that should be considered is the effect of confinement in the bearing stress of the concrete foundation. The effect of added confinement is usually considered by the bearing area ratio. A provision based on the load at failure is given in the American Concrete Institute

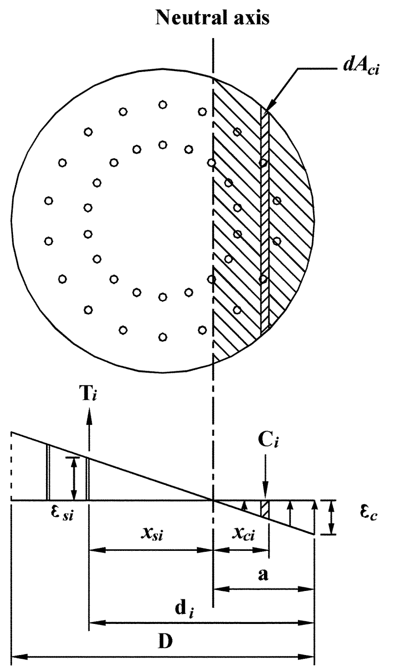

Fig. 17 Segmentation of bearing area and distribution of strains

Code(2002) as follows. The resulting bearing stress at ultimate condition is:

$$f_p = 0.85\phi f_c' \sqrt{A_2/A_1} \le 1.7\phi f_c' \tag{1}$$

in which ϕ is the strength reduction factor equal to 0.70, A_1 is full base plate area, A_2 is full foundation area, and $\sqrt{A_2/A_1}$ is limited to be not more than 2.0.

DeWolf and Sarisley (1980) investigated the relationship between the maximum bearing stress determined from experiments and the bearing area ratio $\sqrt{A_2/A_1}$. They observed that the effects of confinement increase as the eccentricity becomes higher and concluded that it is not correct to use the full plate area for A_1 and the full foundation area for A_2. Therefore, they suggested a method to evaluate the bearing area ratio based on the contact area only. Unfortunately, there exists a very few research on the confinement effect for the design of base plates.

For the design method for circular base plate proposed in this study, an equilibrium approach on the reinforced concrete section will be investigated. This approach is actually analogous to the working stress method mentioned before. In the circular base plate, the consideration of circular geometry is necessary and this can be accomplished by segmentation of circular section in contact with concrete as shown in Fig. 17. Given the axial load, the moment, the plate dimension, and material properties, three unknowns exist, T, a and ε_c. Two equations can be obtained from the equilibrium of axial force and moment. For the third equation, the strain compatibility between the base plate and the foundation is assumed. This assumption seems to be valid for the concrete filled column although it is not consistent with the overhanged part of the base plate. The detailed procedure to determine the concrete stress and bar tensile force is as follows and a computer program was coded for iterative calculation of equilibrium.

Step 1: Assume a neutral axis depth a and concrete strain ε_c.
Step 2: Calculate tensile strains of the bars according to the compatible strain distribution.
Step 3: Calculate the internal moment and axial force.

$$M_{\text{int}} = \sum_{i=1}^{nseg} f_{ci} \cdot x_{ci} \cdot dA_{ci} + \sum_{i=1}^{nbar} f_{si} \cdot x_{si} \cdot A_{si} \tag{2}$$

$$N_{\text{int}} = \sum_{i=1}^{nseg} f_{ci} \cdot dA_{ci} + \sum_{i=1}^{nbar} f_{si} \cdot A_{si} \tag{3}$$

Where *nseg* is the number of arbitrarily divided segments and *nbar* is the number of deformed bars.
Step 4: Check the equilibrium of axial force and moment, i.e.,

$$M_{\text{int}} - M_{applied} = 0 \tag{4}$$

$$N_{\text{int}} - N_{applied} = 0 \tag{5}$$

Step 5: If equilibrium was not achieved, reassume a and ε_c as follows, and go to *step 1*.

if ($N_{\text{int}} > N_{applied}$), then reduce a.
if ($M_{\text{int}} > M_{applied}$), then reduce ε_c.

3.2.2. Material models

As mentioned before, the reinforced concrete section approach has two problems, i.e., the flexibility of the base plate and the confinement effects. It is actually very difficult to define quantitatively the effects of the parameters on the behavior of a base plate, and the followings are assumed.

For the problem of flexibility, the overhanged part of double base plate used in this study seems to have higher stiffness compared to the single base plate that is generally used for a lightly loaded column. Therefore, the strain compatibility between the base plate and the concrete foundation is assumed as acceptable.

For the second problem, a modified concrete model is adopted. Many mathematical models of concrete are currently used in the analysis of confined reinforced concrete structures (Park and Paulay 1975). In this study, the curve proposed by Baker with some modifications is applied. The curve is assumed as a parabola up to a maximum stress then a horizontal branch to a certain strain as shown in Fig. 19(a). The reason to assume a horizontal branch after a maximum bearing stress is that the concrete foundation did not show severe cracks and failure due to confinement effect to the end of the test. The parabola curve is as follows.

$$f_c = f_p\left(\frac{\varepsilon_c}{\varepsilon_m}\right)\left(2 - \frac{\varepsilon_c}{\varepsilon_m}\right) \tag{6}$$

where,

$f_p = 0.85\phi f_c' \sqrt{A_2/A_1}$: maximum bearing stress (6a)

$\varepsilon_m = 0.002 f_p/0.85 f_c'$: the strain that concrete stress arrived at maximum stress (6b)

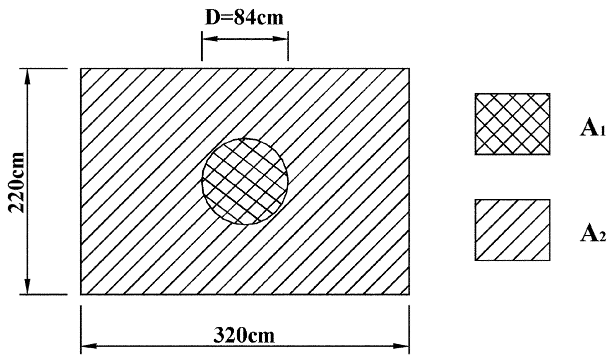

Fig. 18 Bearing area and confining concrete area

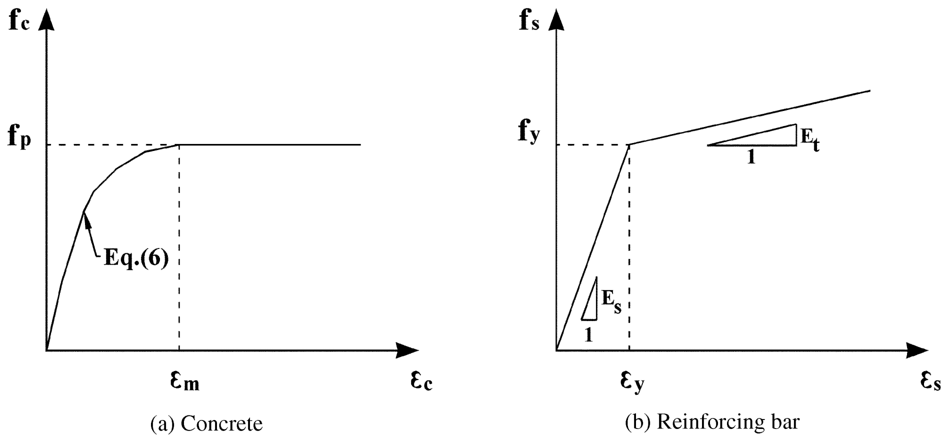

Fig. 19 Material models

In the Eq. (6a), the bearing area ratio $\sqrt{A_2/A_1}$ is assumed as 2.0 according to the ACI code (2002) although it is greater than the limit value 2.0 in this case as shown in Fig. 18. Then, the maximum bearing stress f_p becomes $1.19\,f_c'$ from Eq. (1). For a comparative purpose, the bearing area ratio without considering the limit value is also considered. In this case, the ratio is 3.56 and the maximum bearing stress becomes $2.12\,f_c'$.

Reinforcing steel is modeled as a linear elastic, linear hardening material with yield stress f_y as shown in Fig. 19(b). The behavior of reinforced concrete members is greatly affected by the yielding of reinforcing steel when the structure is subjected to bending moments (Vedo and Ghali 1977). In this study, the yield stress is determined as 40.0 kN/cm^2 from the material tests as shown in Table 1. The tangent modulus after yield is assumed as 1/50 of elastic modulus E_s that is determined from the slope of stress-strain curve between the yield strain and maximum strain at fracture.

3.2.3. Comparisons between predicted and measured results

To evaluate the applicability of the reinforced concrete section approach for the design of the base plate considered in this study, comparisons were made between the predicted and measured results. The predicted values are those obtained from the algorithm based on the reinforced concrete section

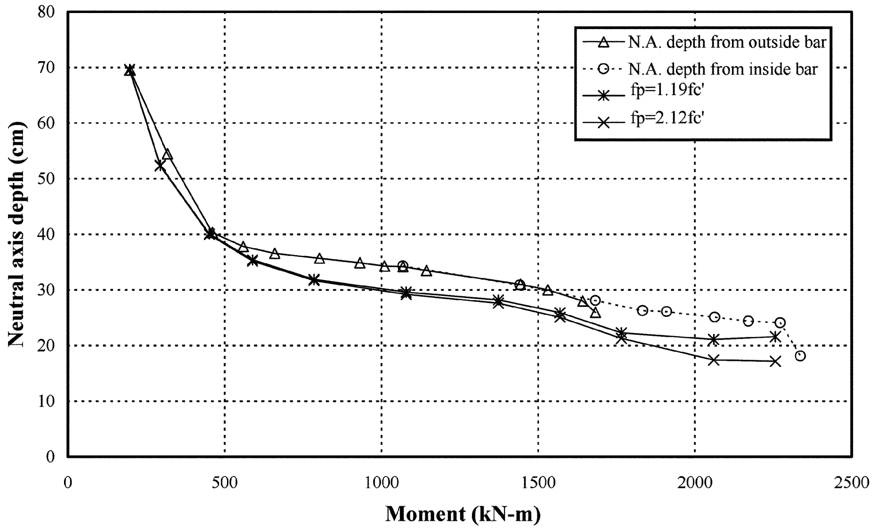

Fig. 20 Neutral axis depths from predicted and measured results

method. In the analysis, the maximum concrete bearing stress considering confinement effect was assumed by Eq. (6).

First, the neutral axis depths are depicted in Fig. 20 for the predicted and measured results. The neutral axis depths from the experiment are estimated from the measured strains at the outside and inside bars, respectively. From the Fig. 20, it is acknowledged that the reinforced concrete section approach a little underestimate the neutral axis depths compared to the experimental results after the moment reached about 500 kN · m. This is considered that, due to the flexibility and local deformation of cantilever part of the base plate, the bearing pressures under overhanged part are less than those under column, consequently moving the neutral axis into the center of the base plate. However, the

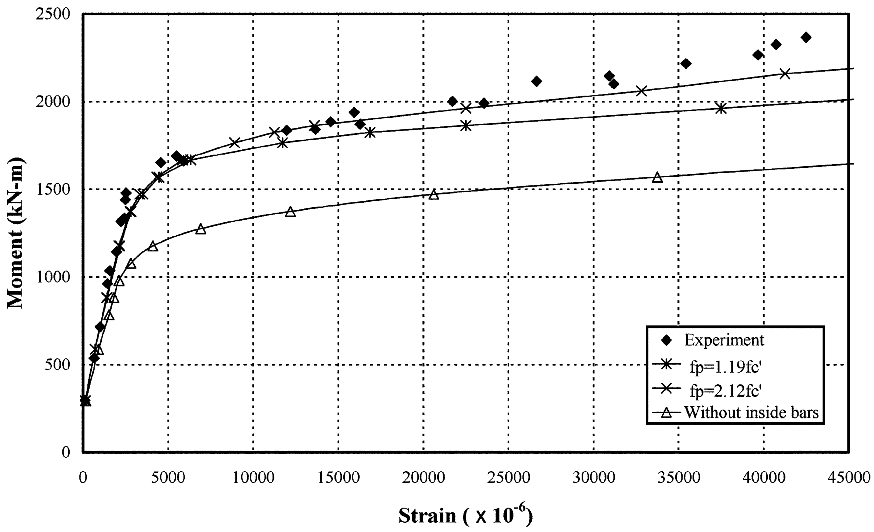

Fig. 21 Moment-bar strain curve

variation of neutral axis depth shows substantial similarity between the predicted and measured values even though there is a certain difference.

The moment-bar strain curves are depicted in Fig. 21 to estimate the ultimate moment capacity of a base plate by reinforced concrete section method. From the figure, it is acknowledged that both cases of assumed concrete bearing stress predict the yield moment 1,620 kN · m well. For the plastic region, the case by assumed concrete bearing stress as $2.12 f_c'$ shows better coincidence with the measured result while the case by $1.19 f_c'$ underestimates the ultimate moment capacity of the base plate system. In the figure, it is also observed that the moment from the test a little exceeds that from reinforced concrete section approach even in the case of assumed concrete bearing stress as $2.12 f_c'$ when the moments are greater than 2,200 kN · m. This is considered by the fact that the bearing stress increases as the eccentricity increases, consequently yielding higher bearing stress as illustrated by DeWolf and Sarisley (1980). In spite of some differences, it is anticipated that the reinforced concrete section approach proposes a practical way to predict the behavior of base plate system.

A base plate without the inside bars is also assumed and the moment capacity is predicted by the reinforced concrete section approach. As shown in Fig. 21, the yield strength of base plate with the inside bars is about 50% higher than that of the base plate without the inside bar.

3.3. Interaction curve approach

By considering the base plate as a column under an axial load and a bending moment, the applicability of the interaction curve to a design method for base plate was also examined. The interaction relationship between a compression strength and a bending strength mainly depends on the yield strength f_y of steel, the strength of concrete f_c', and the steel ratio A_s/A_c. The strain-hardening of a steel bar is generally not accounted for in the interaction curve, thus the bending strength corresponding to a given axial load does not conform to the ultimate strength but to the yield strength of a column.

The interaction curve obtained for the base plate considered in this study is shown in Fig. 22. The curve was determined based on the assumed concrete bearing strength as $1.19 f_c'$ and the yield strength

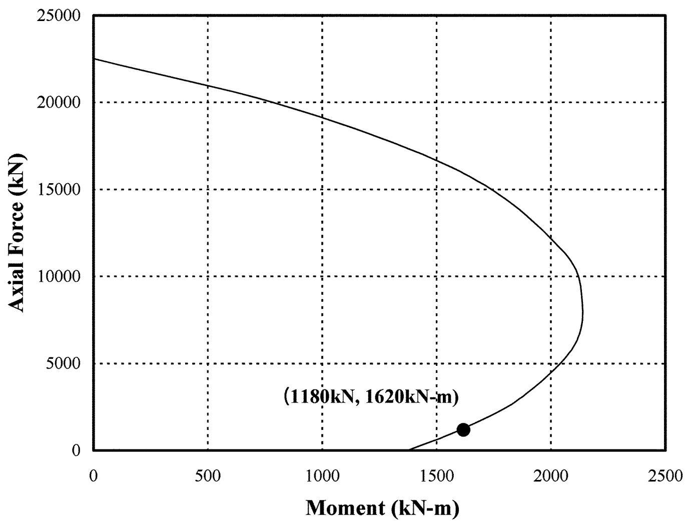

Fig. 22 Interaction curve

of bar 40.0 kN/cm^2. The yield moment 1,620 kN · m evaluated from experiment is exactly located on the interaction curve as shown in the Fig. 22. Therefore, it is anticipated that the interaction curve can be used as an efficient tool to predict the yield strength of a base plate if the bearing strength of concrete considering the confinement effect is properly defined.

4. Conclusions

An experimental and analytical approach has been conducted to investigate the behavior of a base plate with concrete filled circular column. The proposed base plate system is an economical self-anchored system using the deformed reinforcing bars installed at the inside and outside of the column. In order to assess the moment resisting capacity, reversal cyclic loads were applied with the axial load held constant. The measured data showed the inside bars are effective for resisting from both tension and compression force while the outside bars do not withstand compression force at the surface level of concrete foundation.

Some analytical approaches are performed to derive a design method for the plate system. It was recognized that the reinforced concrete section method reasonably evaluates the elasto-plastic behavior and ultimate strength of the base plate if the bearing pressure of confined concrete and tangent modulus of bars are assumed appropriately. Also, it was found that the interaction curve can be used as an efficient tool for the estimation of yield strength of the base plate.

Acknowledgements

Financial support of the Korean ministry of science & technology through National Research Laboratory Program (M1-0203-00-0070) is gratefully acknowledged.

References

ACI Committee 318 (2002), *Building Code Requirements for Structural Concrete(ACI 318-02) and Commentary (ACI318R-02)*, American Concrete Institute, Detroit.

AISC (1986), *Manual of Steel Construction-Load and Resistance Factor Design*, 1st Edn., American Institute of Steel Construction, Chicago.

AISC (1990), *Steel Design Guide 1-Column Base Plates*, American Institute of Steel Construction, Chicago.

DeWolf, J.T. (1978), "Axially loaded column base plates", *J. Struct. Div.*, ASCE, **104**(ST5), 781-794.

DeWolf, J.T. and Sarisley, E.F. (1980), "Column base plate with axial loads and moments", *J. Struct. Div.*, ASCE, **106**(ST11), 2167-2184.

Gaylord, E.H. and Gaylord, C.N. (1972), *Design of Steel Structures*, McGraw-Hill, New York.

Kitada, T., Sakoda, H., Oryu, T., Horie, Y. and Nina, T. (1998), "Ultimate strength of steel bridge pier bases designed as RC structures", *Proc. of the 6th Symp. on Steel Structures*, JSSC, 6, 221-228.

Kontoleon, M.J., Mistakidis, E.S., Baniotopoulos, C.C. and Panagiotopoulos, P.D. (1999), "Parametric analysis of the structural response of steel base plate connections", *Comput. Struct.*, **71**, 87-103.

Park, R. and Paulay, T. (1975), *Reinforced Concrete Structures*, John Wiley & Sons, New York.

Salmon, C.G., Shenker, L. and Johnston, B.G. (1957), "Moment-rotational characteristics of column anchorages", *Transactions*, ASCE, **122**, 132-154.

Stamatopoulos, G.N. and Ermopoulos, J.C. (1997), "Interaction curves for column base-plate connections", *J.*

Construct. Steel Research, **44**(1), 69-89.
Thambiratnam D.P. and Paramasivam, P. (1986), "Base plates under axial loads and moments", *J. Struct. Eng.*, ASCE, **112**(5), 1166-1181.
Vedo, A. and Ghali, A. (1977), "Moment-curvature relation of reinforced concrete slabs", *J. Struct. Div.*, ASCE, **103**(ST3), 515-531.

CC